

## OPTICAL IMAGING AND SPECTROSCOPY OF SUPERFICIAL TISSUE

S. P. MORGAN\*, I. M. STOCKFORD, J. A. CROWE  
and B. R. HAYES-GILL

*School of Electrical and Electronic Engineering  
University of Nottingham  
University Park, Nottingham  
NG7 2RD, UK*

*\*steve.morgan@nottingham.ac.uk*

An overview of three techniques developed by our group for imaging superficial tissue is presented. Firstly, a novel polarized light capillaroscope has been developed for imaging the microcirculation. The capillaroscope has been used to make *in vivo* measurements of sickle cell disorder sufferers with aim of monitoring the polymerization of sickled red blood cells. Secondly, hyperspectral imaging for measuring oxygen saturation is described. The accuracy of such measurements is affected by the non-linear relationship between scattering and absorption and it is demonstrated that polarization techniques can be used to make the relationship more linear, thus improving accuracy. Finally, the use of smart CMOS optical sensors for laser Doppler blood flowmetry is described. A  $32 \times 32$  pixel imaging array with on-chip processing is described and the potential for full field laser Doppler blood flow imaging is demonstrated through measurement on blood flow of tissue before and after occlusion.

*Keywords:* capillaroscopy; laser Doppler; hyperspectral.

### 1. Introduction

Imaging superficial tissue is important for many applications. Examples include inflammatory responses, sickle cell anaemia, tissue engineering, cancer diagnosis, wound healing, skin diseases and plastic surgery. Three techniques for imaging and spectroscopy of superficial tissue are described; polarization sensitive capillaroscopy, hyperspectral imaging for oxygen saturation measurements and full field laser Doppler flowmetry using smart CMOS sensors. Each has their merits for measuring different properties of the microcirculation at different sites on the body.

\*Corresponding author.

## 2. Polarization Sensitive Capillaroscopy

### 2.1. Method

When imaging biological tissue, reflections from the surface of the sample results in degradation of image quality. Video capillaroscopy is a useful technique for imaging the microcirculation on sites where the tissue layer above the moving red cells is relatively thin or is weakly scattering. Examples include the eye, nail fold, lips or the tongue and at these sites the red blood cells can be clearly imaged. However, surface reflections still present a problem and so orthogonal polarization imaging<sup>1</sup> and side stream dark field illumination<sup>2</sup> are commonly used to remove the specular component. In orthogonal polarization imaging co-polar illumination and cross-polar detection is used to remove unwanted surface effects. In side stream dark field illumination, illumination from an annulus around the detector is performed, light then ‘back illuminates’ the tissue of interest, minimizing the surface effects. We have developed a polarized light Monte Carlo model which simulates the imaging response of both orthogonal polarization imaging and side stream dark field illumination to an edge embedded in a scattering medium at different depths. Figure 1 shows the imaging response of both systems to an edge embedded within a scattering medium at a depth of 0.1 mean free paths. This response is consistent over a range of depths. Due to the superior performance of side stream dark field illumination, a polarization sensitive version of this device has been developed (Fig. 2).

Light illuminates the tissue from a ring of LEDs (note the illumination is not polarized) which then back-illuminates the blood cells of interest. If the cells do not alter the polarization properties of the light i.e. they are not polymerized, then randomly polarized light passes through the cells and emerges from the tissue. The presence of linear dichroism (due to polymerization) within the cells means that

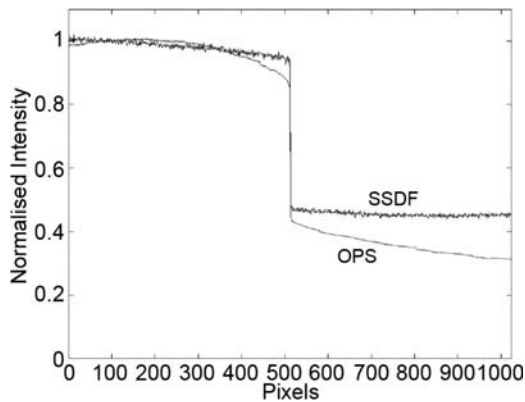


Fig. 1. Imaging response of orthogonal polarization imaging (OPS) and side stream dark field illumination (SSDF) to an edge embedded at a depth of 0.1 mean free paths within a scattering medium.

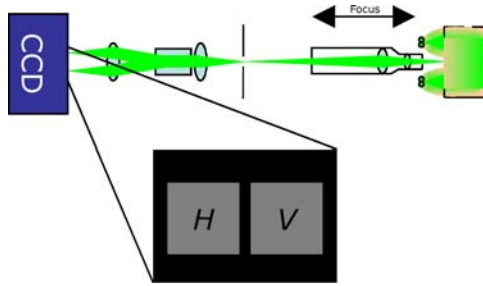


Fig. 2. Polarization sensitive capillaroscope.

the randomly polarized back-illumination has polarization information imposed on it. This information can be extracted by polarization sensitive detection. The light is then imaged by a  $\times 10$  microscope objective onto a CCD camera via a Wollaston prism. The Wollaston prism projects two images (horizontal and vertically polarized) onto the CCD camera. The two images are aligned and distortions are corrected by correlating sub-images. Subtracting the aligned images allows a single polarization difference image to be obtained.

Our main application is in the detection of linear dichroic cells in sickle cell anaemia sufferers. Sickle cell disorder is a genetic disorder that affects the red blood cells. When the cells become deoxygenated they polymerize and become stiff, which results in painful crises and eventual organ damage. Currently there is no *in vivo* assessment of the number of sickled cells. Previous work<sup>3</sup> has shown polarization difference signals of  $\sim 3\%$  *in vitro*.

A device was constructed (Fig. 3) which was used to take clinical measurements on the lower lip of sickle cell disorder sufferers. This site was chosen as it represented the optimum balance between image quality and patient comfort.



Fig. 3. Clinical instrument based upon polarization sensitive capillaroscope.

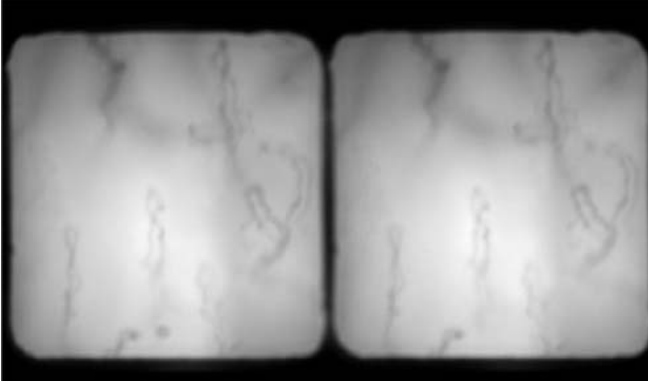


Fig. 4. Horizontally and vertically polarized images from the lower lip of a sickle disorder sufferer.

## 2.2. Results

The sensitivity of the system to differences in polarization from controlled components (e.g. polarizers) was demonstrated to be  $\sim 0.5\%$  which is more sensitive than the 3% difference signal observed *in vitro*. A typical image is shown in Fig. 4. To date, however, the evidence on whether sickled cells can be observed through their dichroism signal is inconclusive. It is possible that the instrument is not sensitive enough, in terms of dynamic range, resolution or image alignment, to observe such effects. It is also possible that there are clinical reasons for dichroic signals not to be detectable *in vivo*. For example the cells may be fully oxygenated on the lower lip and may not be polymerized. This remains an open question and will be the study of future research.

## 3. Hyperspectral Imaging

### 3.1. Method

In the absence of scattering the attenuation,  $A$ , of a sample is linearly related to the total absorption coefficient,  $\mu_a$ . The absorption coefficient itself is a linear sum of the products of the specific absorption coefficients of the constituent absorbers and their concentrations. That is;

$$A = \mu_a d \quad (1)$$

$$\mu_a = \sum_{i=0}^M \alpha_i c_i \quad (2)$$

Where  $A$  is the attenuation,  $d$  is the thickness of the medium (in mm in this paper),  $\mu_a$  is the absorption coefficient in  $\text{mm}^{-1}$ ,  $\alpha_i$  is the molar absorptivity with units of  $\text{L mol}^{-1} \text{mm}^{-1}$  and  $c_i$  is the concentration of the compound in solution, expressed in  $\text{mol L}^{-1}$ .

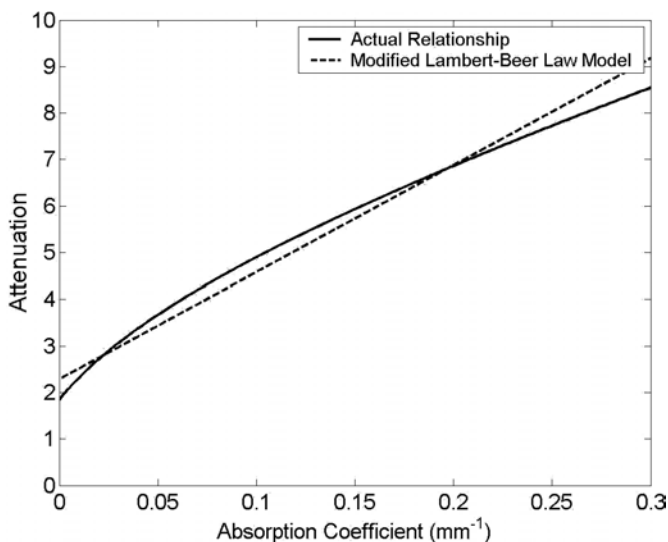


Fig. 5. Non-linear relationship between attenuation and absorption in the presence of scattering.

However in the presence of scattering the relationship between attenuation and absorption becomes non-linear and errors are introduced into the interpretation of the measurements (Fig. 5). This non-linearity produces errors in spectrophotometric measurements when the Lambert-Beer is assumed, even if an offset to allow for  $A_s$  is included as a model of the form  $A = A_s + \mu_a d$ .<sup>4</sup> Therefore techniques that could overcome the effects of scattering so that accurate quantitative spectroscopy can be performed would be of widespread use.

An approach that can be easily applied to reduce the effects of scattering is polarization subtraction.<sup>5</sup> Weakly scattered light maintains its original polarization state and a simple subtraction of co- and cross-polarization channels results in extraction of the weakly scattered component. In spectroscopy this results in the relationship between attenuation and absorption becoming more linear.

Two absorbing species with a concentration ratio of 2 within a scattering medium were simulated using Monte Carlo simulations. Fits to the modified Lambert-Beer Law were carried out to estimate the ratio.

### 3.2. Results

For the case shown in Fig. 6, two wavelengths were fixed while a third wavelength was varied in the fitting routine. Figure 6 compares estimates of the concentration ratio ( $R'$ ) obtained using polarized light data (both circular and linear) and total intensity measurements as the third wavelength is varied. The results demonstrate that linear polarization is most effective at making the relationship between attenuation and absorption more linear and results in more accurate estimates of the ratio of two absorbers  $R'$  over a range of wavelengths.

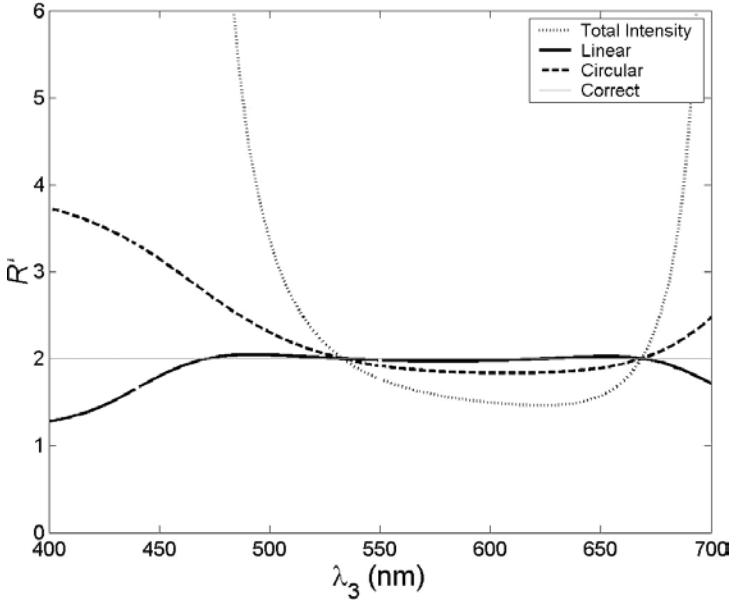


Fig. 6. Estimate of the concentration ratio of two absorbers via fits to the modified Lambert Beer Law (actual ratio = 2).

## 4. Full Field Laser Doppler Flowmetry

### 4.1. Method

Recently, full field laser Doppler perfusion imaging has been implemented using a commercial CMOS image sensor coupled with a digital signal processor (DSP).<sup>6</sup> The advantage over scanning laser Doppler imaging is that movement artifacts are reduced and the scanning speed of the system is increased due to the absence of moving scanning components. However, a data bottleneck exists between the camera and the signal processing unit as all data needs to be transferred to a separate processing unit to be processed and compromises have to be made to achieve acceptable performance. For example in their most recent work, Serov *et al.*<sup>6</sup> have demonstrated full field laser Doppler imaging but employ a sampling frequency of 8 KHz, usually a sampling frequency of  $\sim 40$  kHz is considered appropriate for laser Doppler blood flowmetry. Furthermore, as a general purpose CMOS image sensor is used, the capabilities and specifications of the camera are set by the manufacturer.

A custom made camera design offers several advantages over commercial cameras as the specifications can be tailored to the signals of interest. An important advantage of custom made sensors is that on-chip processing allows the data bottleneck that exists between the photodetector array and processing electronics to be overcome, as the *processed* data can be read out from the image sensor to a PC

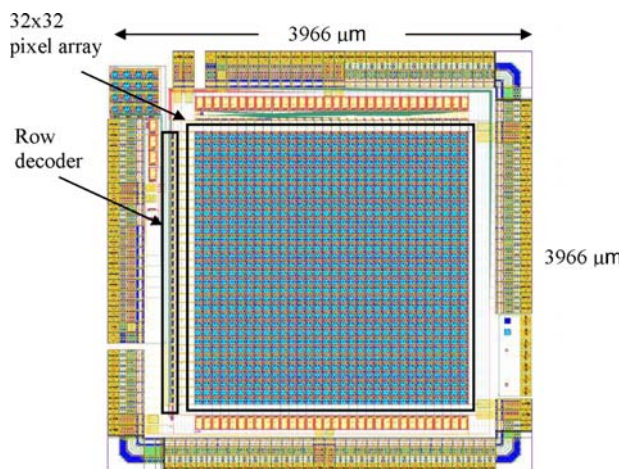


Fig. 7. A  $32 \times 32$  CMOS sensor array. At the pixel level is a transimpedance amplifier, a hysteretic differential amplifier and an anti-aliasing filter.

or display at a low data rate. This provides the potential for a large number of parallel processing channels to be implemented each being sensitive to high frequency fluctuations but with a low data readout rate from the sensor.

One sensor design is shown in Fig. 7. This consists of an array of  $32 \times 32$  photodiodes with analogue on-chip processing. Each pixel contains a photodiode, transimpedance amplifier, a hysteretic differential amplifier and an anti-aliasing filter. For this sensor the frequency weighted filter used to calculate the blood flow is implemented on a PC. In other variations of our designs we have also implemented a  $16 \times 1$  array with mixed analogue and digital processing, and a  $4 \times 4$  array with all analogue on-chip processing. The experimental set up used to obtain blood flow imaging is shown in Fig. 8. Light from a HeNe laser ( $P = 30 \text{ mW}$ ,  $\lambda = 633 \text{ nm}$ ) illuminates an area of tissue which is then imaged back onto the CMOS array. Measurements were taken of an unoccluded finger, an occluded finger and a tissue phantom containing no moving particles.

#### 4.2. Results

Here we simply provide a single result demonstrating that between frames a blood flow change can be observed. Figure 9 shows ten measurements taken on an unoccluded finger, an occluded finger and a static tissue phantom at a single pixel in the array. For each measurement, the finger is removed and then re-inserted in front of the beam. The flow signals from the unoccluded finger, the occluded finger and the tissue phantom can be easily differentiated and this provides an indication of the dynamic range of the system corresponding to a high flow value, biological zero and electrical zero respectively.

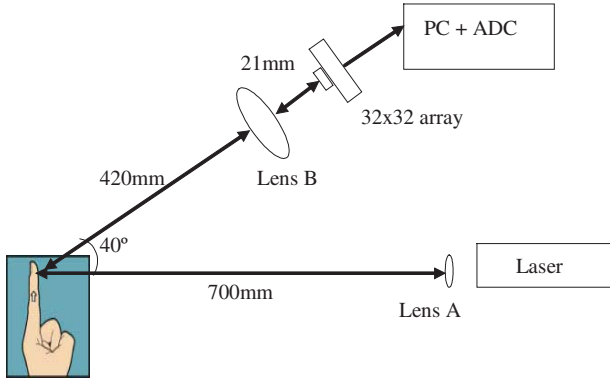


Fig. 8. Experiment configuration. Lens A,  $f = 10$  mm, lens B,  $f = 20$  mm, both 25 mm diameter. Light from a HeNe laser ( $\lambda = 633$  nm, power = 30 mW) diverges from lens A and illuminates a circular area of  $\sim 50$  mm diameter on the tissue.

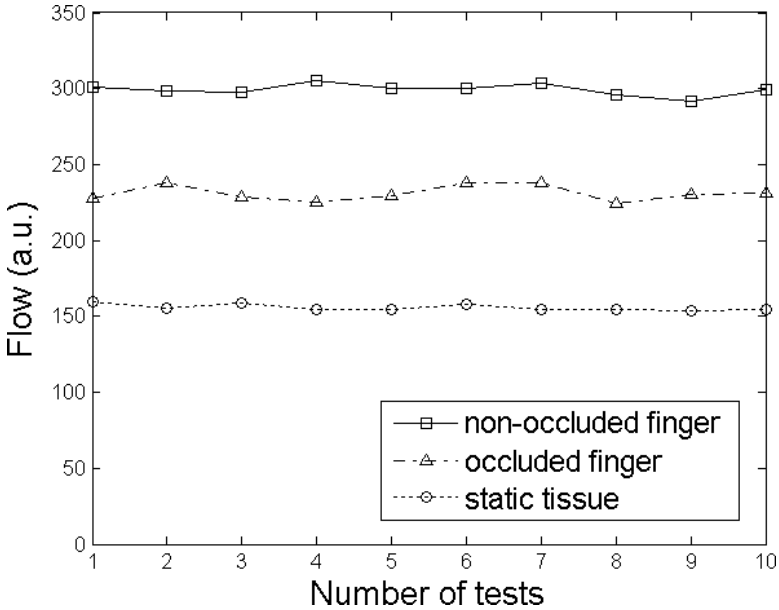


Fig. 9. Comparison of measurements taken on a non-occluded finger (upper line) occluded finger (middle line) and a static tissue phantom (lower line).

### 5. Conclusions

An overview of three novel methods developed by our group for imaging superficial tissue has been provided. The first, a polarized light sensitive capillaroscope has been shown to be capable of detecting 0.5% differences in polarization images. Although 3% polarization difference signals have been observed, *in vitro*, to date



the evidence is inconclusive as to whether it is an appropriate device for monitoring sickle cell disorder *in vivo*. The second methods combines hyperspectral imaging with polarized light imaging to make the relationship between absorption and attenuation more linear. When a fit of the modified Lambert-Beer law is applied, measurement of the ratio of two absorbers becomes more accurate using linear polarization than simply applying total intensity measurements alone. This has important applications in imaging the oxygen saturation of the skin. Finally the use of custom made smart CMOS optical sensors for laser Doppler blood flow imaging has been demonstrated. Differences between the laser Doppler blood flow signals from an unoccluded finger, an occluded finger and a tissue phantom with no moving particles can be easily differentiated. This demonstrates the feasibility of progressing to larger imaging arrays in the future.

### Acknowledgments

This work has been funded by Department of Health (Neat Programme), Big Lottery Fund (via Sickle Cell Society), Royal Society, and the Engineering and Physical Sciences Research Council. Thanks also to M Pickstone, JG Walker, GF Clough, MK Church, D He, PI Rodmell, Q Gu, C Kongsavatsak, B Lu, G Stabler, NBE Sawyer, N Hoang, L Bo and DE Morris.

### References

1. W. Groner, J. W. Winkelman, A. G. Harris, C. Ince, G.J. Bouma, K. Messmer and R. G. Nadeau, 'Orthogonal polarization spectral imaging: a new method for the study of the microcirculation,' *Nat. Med.* **5**(10), 1209–1213 (1999).
2. C. Ince, 'The microcirculation is the motor of sepsis,' *Crit. Care* **9** (suppl 4), S13–S19 (2005).
3. D. A. Beach, C. Bustamante, K. S. Wells and K. M. Foucar, 'Differential polarization imaging. III. Theory confirmation. Patterns of polymerization of hemoglobin S in red blood sickle cells.' *Biophys. J* **53**, 449–456 (1988).
4. R. N. Pittman and B. R. Duling, 'Measurement of percent oxyhemoglobin in the microvasculature,' *J. Appl. Physiology* **38**, 321–327 (1975).
5. B. Lu, S. P. Morgan, J. A. Crowe and I. M. Stockford, 'Comparison of methods for reducing the effects of scattering in spectrophotometry,' *Applied Spectroscopy* **60**, 1157–1166 (2006).
6. A. Serov, B. Steinacher and T. Lasser, 'Full-field laser Doppler perfusion imaging and monitoring with an intelligent CMOS camera,' *Opt. Express* **13**, 3681–3689 (2005).